Egypt. J. Chem. **Vol. 68**, No. 7 pp 285-301 (2025)

Egyptian Journal of Chemistry

http://ejchem.journals.ekb.eg/

A Novel Approach Using Polyamine and Copolymeric Sealants in Water-Based Mud Systems

Eissa M. Shokir, Abdel Sattar Dahab, Mostafa A. Seleem*

Department of Mining, Petroleum and Metallurgical Engineering, Cairo University, Giza, 12613, Egypt

Abstract

In the Egyptian Western Desert's Northern region, drilling in the intermediate sections using water-based muds (WBM) often results in wellbore instability due to microfracture shale formations containing a high percentage of Smectite, leading to pack-offs and tight holes. Although non-aqueous drilling fluids (NAF) are successful, they are not always practical due to environmental concerns, logistics, and costs. Therefore, a WBM system that is environmentally friendly has become mandatory where multiple investigations were conducted, including Cation Exchange Capacity (CEC), Scanning Electron Microscope (SEM), Shale Particle Disintegration Test (SPDT), Accretion Test, Bulk Hardness, and Linear Swell Meter (LSM) tests, to understand the shale mineral composition and evaluate shale stability in the presence of different test fluids. The research resulted in developing a new drilling fluid system called NanoSeal-KP, which is environmentally friendly and incorporates a polyamine-based inhibitive additive with a copolymeric nanoparticle sealant agent to minimize shale fluid interaction and pore pressure transmission, respectively. Furthermore, a solid lubricant additive guarantees premium lubricity for drilling optimization. The study showed that the drilling fluid's performance is comparable to NAF, offering a promising alternative that has zero impact on Health, Safety, and Environment, such as exposure to toxic chemicals, fire hazards, pollution, and soil contamination.

Keywords: Wellbore Stability; Polyamine; Nano-Particle Sealant; Chemical Rock Fluid Interaction; HP-WBM.

1. Introduction

Ensuring wellbore stability in shales has been a significant concern for oil-field engineers since oil and gas well drilling began[1]. When drilling in shale formations using water-based muds (WBM), the reactive shale interactions with the fluid phase can change the physicochemical and mechanical properties of the shale. This leads to the degradation of the shale matrix texture and results in wellbore instability[2, 3]. It is estimated that up to 20% of the total well drilling cost is lost due to wellbore instability problems, and up to 90% of instability problems are encountered when drilling shale formations[4]. Shale formations drilled worldwide contain high clay content and are highly sensitive to WBM, which generates associated wellbore instability problems [5].

In 1993, Mody and Hale delved into the physio-chemical interactions between mud and shale, intending to create a model that could enhance borehole stability. They found that water movement is primarily governed by two mechanisms: the difference in hydraulic pressure between wellbore pressure and pore pressure, and the difference in chemical potential between drilling fluid and pore fluid. The activity of drilling fluid is a crucial factor in determining the influx or outflux of water from shale formations, as it impacts the stresses around the borehole, rock strength, and pore pressure [6].

In 2013, Sone and Zoback conducted a series of mechanical experiments on various types of shales, each with different mineralogies and clay contents. These shales are known as reservoir shales, as they contain kerogen volume along with the clay. The tests included hydrostatic and triaxial compressive strength tests, and the researchers found that Poisson's ratio didn't correlate with clay content while Young's modulus did, with a general trend of decreasing elasticity as clay content increased. Furthermore, unconfined compressive strength was found to decrease as clay content increased.

These and other observations led Sone and Zoback to conclude that the ductility and brittleness of shales are dependent on the sample's composition and anisotropy. As clay content increases, shale rock tends to become more ductile [7].

Water-sensitive shale tends to absorb water when exposed to traditional water-based drilling fluids. Depending on its chemical characteristics, this can cause the shale to swell or disperse. As a result, issues such as bit-balling, cuttings disintegration, borehole collapse and enlargement, high torque and drag, tight holes, stuck pipes, poor log quality, and poor cement jobs can occur. These issues lead to increased exploration and production costs and delayed production dates.[4, 8-10]

The four main clay groups found frequently in shale formations are kaolinite, smectite, illite, and chlorite. In general, shales with high percentages of kaolinite tend to disperse and disintegrate, while those with high percentages of smectite tend to swell and increase in volume when they come in contact with aqueous fluids, especially fresh water[11]. Factors such as clay structure, cation exchange capacity, fluid type and salinity, cation types and positions, and geomechanics from a mechanical point of view play a role.

In the oil drilling industry, reducing the coefficient of friction (COF) is a critical factor in preventing wear between BHA and casing strings, minimizing vibration, increasing bit life, improving rate of penetration (ROP), and improving overall drilling efficiency. NAF has significant benefits in shale stability and lubricity. But, it also has several drawbacks, such as high costs, environmental limitations, logistical challenges, disposal issues, negative effects on reserve oil drilling and completion, and health and safety concerns. Therefore, it is important to create a WBM that performs similarly to NAF due to its eco-friendly

---

*Corresponding author e-mail: mmohamed01@slb.com (Mostafa Ahmed Seleem)

Receive Date: 21 January 2024, Revise Date: 06 March 2024, Accept Date: 17 April 2024
DOI: 10.21608/ejchem.2024.264461.9223

nature and high-performance characteristics, as suggested by Ahmed et al. (2017) [12]. Researchers aim to achieve the performance of NAF systems using a WBM, identifying shale stabilization and lubricity properties as key design targets.

Many efforts are being made to develop wellbore stabilizers, shale-swelling inhibitors, and pressure transmission sealants, with maximum performance without affecting drilling fluid properties. This study fully characterized well-preserved cutting samples from shallow, medium, and deep shale formations in the Northwestern Desert of Egypt in terms of structure, texture, mineralogy, and shale reactivity with drilling fluids. The shale sample was first characterized by describing bedding and sedimentary structures, color, and existing fractures. The cation exchange capacity (CEC) and Scanning Electron Microscope (SEM) analysis were used to assess shale reactivity with drilling fluids. To evaluate the applicability of test fluids, including freshwater, KCL-polymer, High-performance WBM, NanoSeal-KP WBM, and NAF, the Shale Particle Disintegration Test (SPDT), Linear Swelling Test (LSM), Bulk Hardness Test, and Accretion Test were used.

The approach of using actual shale formations for experiments is holistic and effective since it covers many geological characteristics of the rock samples, including the type of clays, amounts, and reactivity. This study provides an innovative insight into selecting the efficient stabilizer for this clay-rich formation, which is essential to minimize formation damage and improve recovery mechanisms.

This study discusses the results and integration of the chemical instability analysis and lab experiments to develop an advanced drilling fluid system. The study outlines implications for future research and practical applications.

1. Experimental

This section describes the experimental work carried out to examine the effect of drilling fluid on wellbore stability. Shale samples from well (X) were subjected to laboratory tests to assess their mineralogy and chemical reactivity, as depicted in Figure 1. The study involves three main stages. The first stage involves API fluid design and testing. The second stage includes shale characterization, such as SEM and CEC analysis. The third stage involves shale-fluid interaction tests, including Shale Particles Disintegration Test (SPDT), Accretion Test, Bulk Hardness Test, Linear Swell Meter Test (LSM), and Lubricity Optimization. Additionally, the drilling fluids utilized in the experiments underwent analysis to determine their composition, pH, rheology, fluid loss, and other factors.

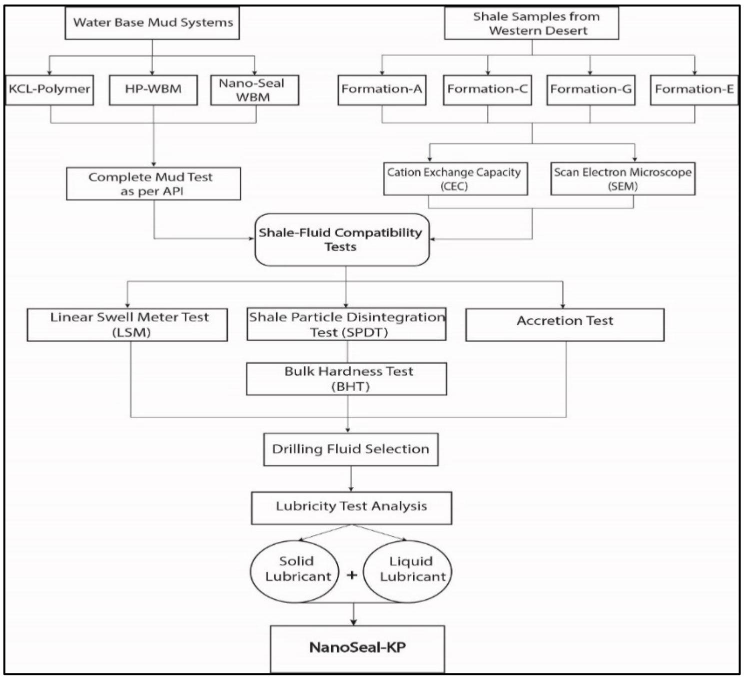

Figure 1: Flow procedures for conducting the chemical wellbore stability study experimental work.

2.1. Shale preservation techniques

Due to their swift decline and improper storage conditions, causing shales to become unsaturated, data collection through the inspection of cuttings has often been inadequate or entirely unsuccessful. Recent studies suggest that the shales exhibit unsaturation phenomena upon dehydration, leading to false test results due to the incorporation of capillary pressure artifacts [13].

In addition, if shales become unsaturated during retrieval or handling, it can drastically alter their mechanical properties, like strength and elastic properties [14]. By compressing the air within the capillaries of unsaturated shale, water can cause severe damage to the structure of the rock mass. Even minimal desaturation during management or preservation can alter the shale matrix and, in turn, affect the shale's behavior [15-17].

It is also important to remember that shale that has been altered during management will not normally react even after being returned to its original hydration conditions. When compared to cuttings maintained in their original hydration conditions, altered shale tends to swell at an abnormally high rate. To maintain its native qualities and provide reliable results, shale must be handled and stored with the utmost care [18, 19].

1.2. Shale Drilling and Handling

An inverted emulsion mud was chosen to reduce the likelihood of shale destruction while drilling. It weighed 10.0 lb/gal with barite and included roughly 62% Diesel and 21% of an emulsified internal phase of 0.87 activity $CaCl_2$ brine that had been mixed with $CaCl_2$ of 96% purity. Calcium soaps were the emulsifiers. The samples were collected as soon as the cuttings were brought to the shakers and stored in plastic bags, then in sample bags to provide an additional layer of protection, with the formation name and depth noted on the outside of each bag (see Figure 2). This method kept the cuttings hydrated and prevented them from drying out or dehydrating during transport and storage.

Figure 2: Group of shale cuttings that are stored in plastic bags, with a sample bag placed alongside them.

1.3. Shale Formations Description

The subsurface formations can be described as follows:

Formation A: The lithological units include Shale (SH) and Limestone (LST). Shale is dark gray with occasional brownish hues and a moderately to finely laminated and thinly bedded structure. Limestone is off-white with a soft to moderately hard texture and contains argillaceous components with glauconite intra-clasts.

Formation C: Comprises shale and limestone. Shale is typically dark gray with hints of brown and a moderate to thinly bedded structure. Limestone is grayish white to off-white with a moderate to soft texture and contains microcrystalline structures, with siliceous and argillaceous composition and glauconite intra-clasts.

Formation G: Comprises shale (SH) and siltstone (SLST). Shale layers exhibit a range of shades of gray and possess a soft to moderately firm texture with sub-blocky to sub-fissile and occasionally blocky structures. Siltstone intervals range from sandy to sub-blocky, with moderate to soft textures.

Formation E: Consists of shale, sandstone, siltstone, and unconsolidated sandstone. Shale sections are typically light to dark gray with a moderately firm texture. Sandstone intervals exhibit a range of hues, such as tannish white, white, and moderate shades of reddish-brown, with a moderate to hard friable texture. Siltstone sections show grayish-white, brownish-white, and light gray coloration, with a moderate to firm texture and finely laminated to thinly bedded structures.

1.4. Cation Exchange Capacity (CEC)

A Cation exchange capacity test (CEC) was conducted to determine the reactivity of the shale sample by measuring the exchangeable cations. Since shale layers are negatively charged, they need to have cations such as sodium, potassium, or calcium to be neutral in charge. The tendency of the shale to exchange those cations can indicate the shale's reactivity. Higher CEC values indicate higher shale reactivity [20].

One gram of the shale sample was ground to a particle size of less than 75 microns. Then, the sample was mixed in an Erlenmeyer flask with 10 ml of de-ionized water, 15 ml of hydrogen peroxide, and 1 ml of sulfuric acid (5N). The sample was boiled gently for 10 minutes. After that, it was cooled down to room temperature and diluted with water to a volume of 50 mL. Titration started by adding methylene blue solution in increments of 0.5 mL while being stirred with a magnetic stirrer. The flask contents were swirled after each addition of the methylene blue solution, and one drop is transferred from the solution with a stirring rod and placed on filter paper. The titration endpoint was reached when the dye appeared as a faint blue ring [21].

1.5. Scanning Electron Microscope (SEM)

The shale samples were characterized using the Scanning Electron Microscope (SEM) as the third imaging technique. In this method, a focused beam of electrons is used to generate images that study the topography of the sample. The SEM images were produced using the instrument model JSM-IT200, with resolutions ranging from 10 to 30 Kx. To prepare the SEM sample, a small amount of the shale rock was ground and fixed onto the sample holder, followed by gold coating to enhance its conductivity, reduce charging effect and thermal damage, and amplify the secondary electron signal. For sample preparation, the sample holder was cleaned with ethanol, and two-sided tape was glued on it. The sample was placed on the tape and coated in the coating machine, which features a cathode made of gold, an anode, and the sample stage. In the sputter coating process, when argon (an inert gas) is energized, gold atoms are dislodged. These atoms then collide with gas atoms and deposit on all inner surfaces of the machine, including the sample. This technique is referred to as sputter coating [22].

1.6. Shale Particle Disintegration Test (SPDT)

The SPDT test is a method used to evaluate the tendency of shale samples to disperse when exposed to drilling fluids. The test involves rolling 20 g of shale in a hot-rolling cell with 350 cm^3 of drilling fluid being tested. After 16 hours of hot rolling at 196 °F, the shale cuttings are collected on a screen and washed with inhibited KCl brine (3.5 %wt). The cuttings are then dried in the oven at 220°F before being weighed to determine the percentage of cuttings recovered. Results are presented as a percentage of cuttings recovery, with a higher percentage indicating quality inhibition against dispersion and a reduced amount of cuttings dispersing [21]. The recovered shale percentage is calculated using Eq. 1.

$$\%\ \text{Recovered Shale} = 100 \times \frac{\text{Mass of dry recovered shale}}{\text{Mass of initial shale corrected for moister content}} \qquad \text{Eq.1}$$

1.7. Accretion Test

In the past, HP-WBMs' inability to meet OBM standards was largely attributed to "bit-balling," a phenomenon where partially hydrated shale cuttings become compressed onto the drilling assembly, resulting in a suboptimal rate of penetration (ROP) and other drilling performance issues [23]. Accretion and its related complications are highly intricate and problematic, with contributing factors such as the type of shale formation being drilled, drilling fluid, lubricity, and other drilling parameters like rate of drilling. A straightforward laboratory test for accretion involves placing a steel bar of fixed size and weight in a cell that contains the test fluid and a specific weight of shale cuttings. The cell is then placed in a rotating oven for a suitable period, and after the set time, the cells are taken out of the oven, and the steel bars are removed and photographed. The amount and percentage of accretion are determined by removing, drying, and weighing the accreted shale cuttings that have accumulated on the steel bar [24].

1.8. Bulk Hardness

The purpose of this test is to determine the hardness of a shale sample that has been exposed to a test fluid. The hardness of the shale sample is indicative of the inhibitive properties of the drilling fluid being evaluated [25]. A shale inhibitor can significantly reduce the clay's capacity to absorb water from the drilling fluid's aqueous environment, resulting in good shale inhibition and stronger wellbore strength during the drilling process. This can lead to trouble-free drilling of water-sensitive shale formations. To perform this test, a bulk hardness tester, as shown in Figure 3, is used.

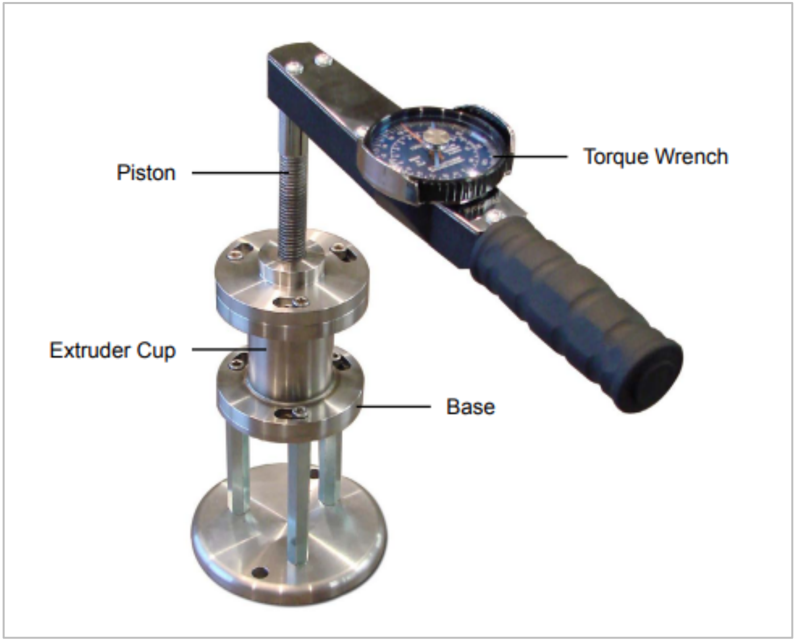

Figure 3: Bulk hardness tester

A fixed size and amount (30.0 g) of shale cuttings are hot rolled in the test fluid at 150°F for 16 hours. After hot rolling, the shale cuttings are sieved (1mm), washed with brine, and placed into a bulk hardness tester. The shale cuttings are then extruded through perforated plates using a torque wrench, with the torque required for extrusion measured after each turn in compression. Depending on the shale's hardness and the efficiency of the shale inhibitor, the torque may reach maximum torque (250 psi) and form a disc, or it may continue to extrude and form ribbons [24].

1.9. Linear Swell Meter (LSM)

The swelling test is a valuable tool for assessing the water-absorption tendencies of shale samples when subjected to drilling fluids. This method is especially helpful when the rock samples comprise a substantial proportion of swelling clays. By measuring the degree of swelling that occurs in the shale when it encounters the fluid, this test provides insight into the shale's responsiveness to the fluid [26].

To conduct the LSM test, we utilized the OFITE Dynamic Linear Swell Meter 150-80-1 (Figure 4) in accordance with the manufacturer's instructions [27]. The test was carried out dynamically at various temperatures for a duration of 2160 minutes. We created the LSM pellets using the OFITE Compactor, compacting a 20-gram powdered rock sample that was sieved through a 200-mesh screen for 1.5 hours at 10000 psi. The resulting pellets were then utilized in the LSM testing and placed into the LSM equipment following the manufacturer's guidelines. Once the pellets were in place, we added 200 cm3 of fluid to the container and initiated the test.

Figure 4: Dynamic linear swell meter [27]

2. Results and Discussion

In this section, we will showcase the findings from our thorough analysis of the experimental work. This includes an in-depth look at shale characterization, which involves examining Cation CEC and SEM data. Additionally, we will discuss the various drilling fluid formulations that were utilized, such as KCl-polymer Mud, High Performance WBM, and Nano-Saeal KP Water Base Mud, as well as their corresponding specifications (Complete Mud Check as per API 13 b). Lastly, we will delve into the interactions between shale rock and drilling fluids, as revealed through SPDT, LSM, Bulk Hardness, and Accretion Test.

3.1. Cation Exchange Capacity (CEC)

The shale samples were subjected to testing, and the endpoint was recorded for each of them. Specifically, for Formations A, C, G, and E, the endpoint was reached at 12 ml, 12 ml, 8 ml, and 15 ml, respectively, which are measured in milliequivalents per 100 g of clay, as shown in Figure 5. Each drop on the paper represents an addition of 0.5 ml of Methylene Blue solution. The faded blue ring indicated each formation's endpoint. This endpoint suggests that formation (A) has a higher tendency to cation exchange capacity and, in turn, a high tendency to swelling. The high CEC result can indicate the high Smectite content of the (A) shale sample, while, on the other hand, low Illite and Kaolinite content are present in the shale sample.

Following (E) formation, moderate cation exchange capacity was demonstrated by samples (A) and (C), corresponding to decreased Smectite content compared to sample (E). Sample (G) exhibited the lowest CEC value in all samples, indicating a relatively lower reactivity and swelling potential (Figure 6). However, the CEC value of the sample (G) still suggests a relatively high potential for swelling and instability.

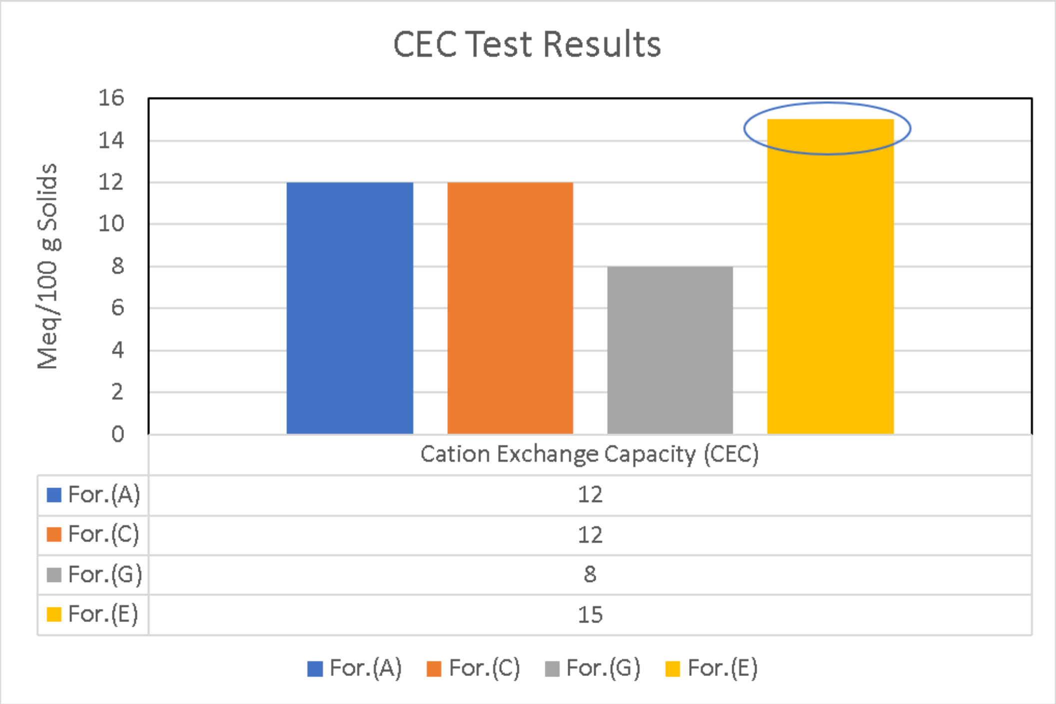

	Cation Exchange Capacity (CEC)
■ For.(A)	12
■ For.(C)	12
■ For.(G)	8
■ For.(E)	15

Figure 5: Cation exchange capacity test results for formation a, c, g, and e

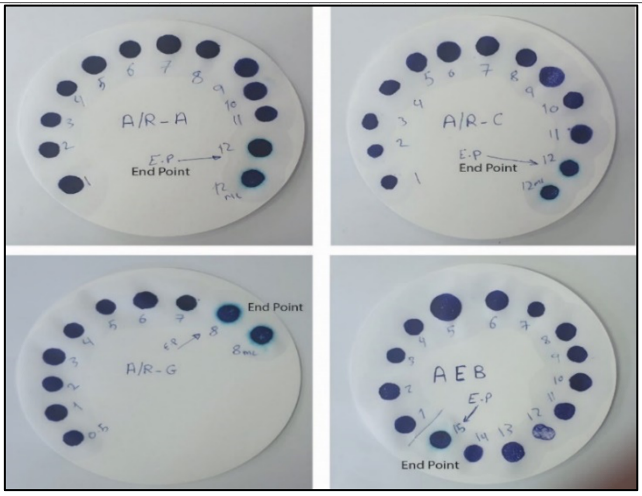

Figure 6: Results of the CEC determination using the methylene blue test (MBT)

3.2. Scanning Electron Microscope (SEM)

In the SEM images of formation (A, C, G, and E), the clay particles dominate and are easily distinguishable as sheets covering the entire area, as depicted in Figure 7-10, where white arrows indicate plate-like clays and quartz, while yellow arrows indicate micro fractures. Although present in minor amounts, quartz grains can also be detected. The high-resolution image reveals the presence of potential micro-cracks and micro-pores with an aperture of up to 0.5-1.0 µm. Additionally, a small quantity of organic matter pores can be observed. While interparticle pores are observable in appreciable quantities, intraparticle pores are absent due to the low porosity that is typical of clay-rich samples.

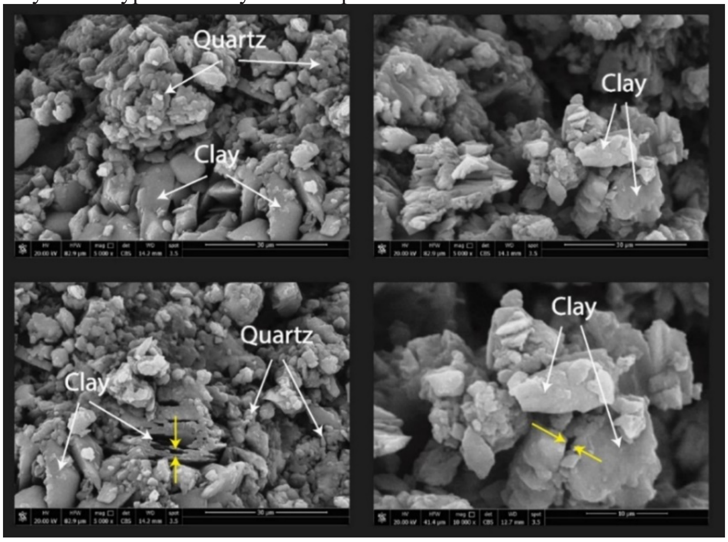

Figure 7: SEM image of the examined sample for formation (A).

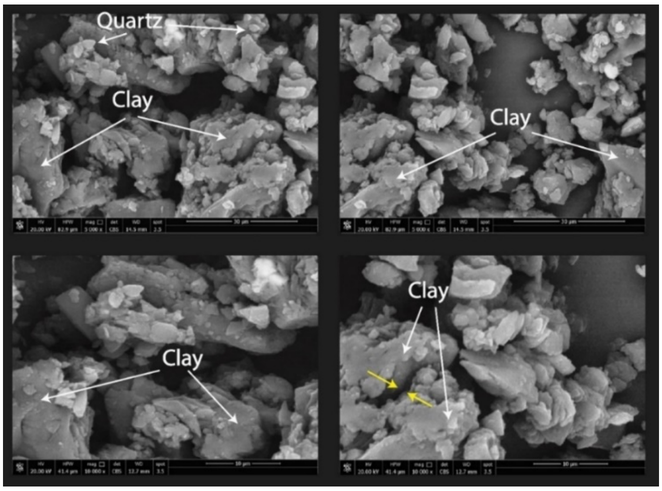

Figure 8: SEM image of the examined sample for formation (C).

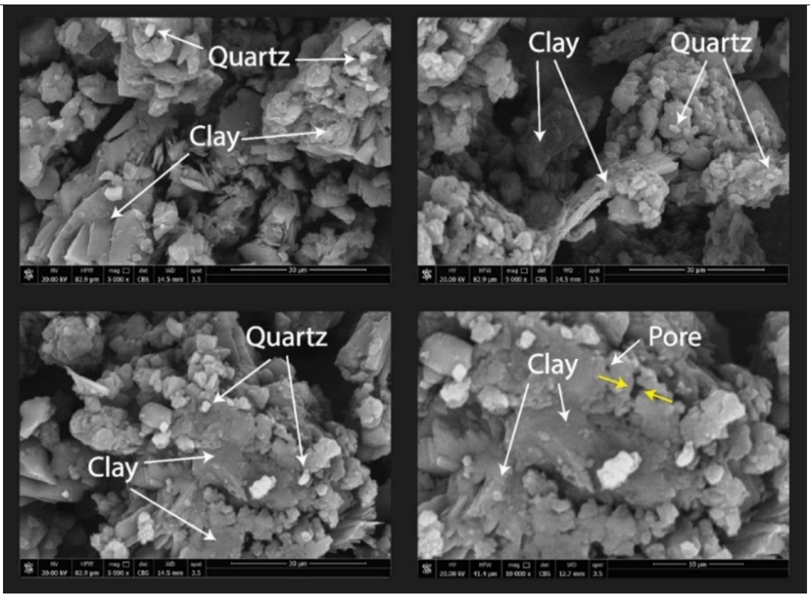

Figure 9: SEM image of the examined sample for formation (G).

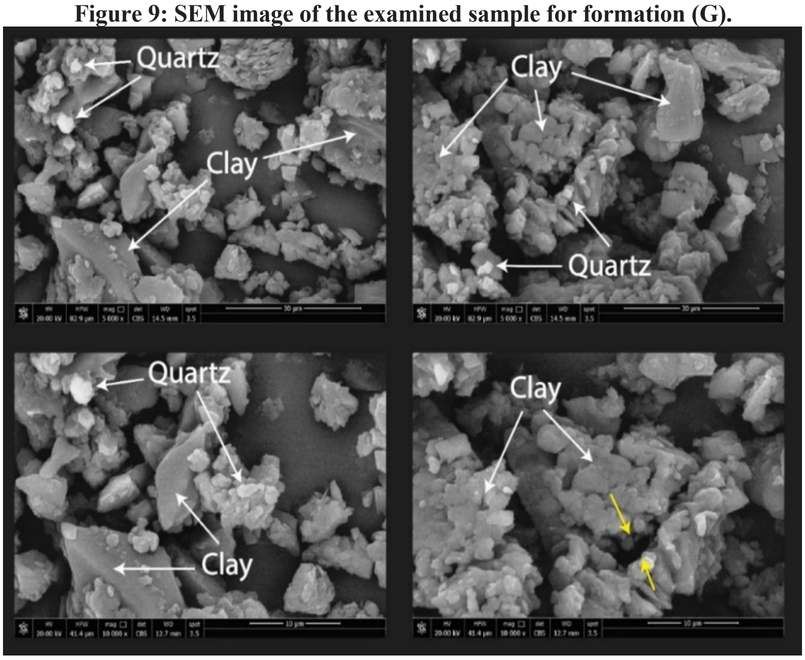

Figure 10: SEM image of the examined sample for formation (E).

3.3. Fluids Preparation and Characterization

Drilling Fluids were prepared and tested following the API recommended practices [28, 29].

Fluid Design

To conduct the research, a thorough analysis of three distinct Water-Based mud systems was carried out. These systems were meticulously studied and analyzed: KCl-Polymer mud, High-Performance Water-Base Mud (HPWBM), and NanoSeal-KP mud. The study also included the Fresh Water and Low Toxic OBM (LTOBM). For a better understanding of these systems, Table 1 provides the composition details, while Table 2 lists their respective properties.

3.4. Shale Particle Disintegration Test (SPDT)

The Shale Particle Disintegration Test (SPDT) is a crucial testing method for assessing the stability of shale formations. This study collected several rock samples from Well X at depths of 4,500 ft, 5,880 ft, 7,110 ft, and 11,670 ft – representing Formations A, C, G, and E, respectively. The collected formations were subjected to SPDT using various fluids, including KCL-Polymer, HPWBM, NanoSeal-KP, fresh water, and LTOBM see Tables 3-6. The percentage of particle recovery was then recorded for each test, with higher recovery rates indicating less shale reactivity and, consequently, less dispersion in the well.

The results of the SPDT were quite interesting. When tested with fresh water, the recovery percentage was found to be quite low, with less than 50% of particles recovered across all rock samples. However, drilling fluids increased recovery rates, with the best results observed using the NanoSeal-KP fluid. In fact, the recovery percentage ranged from an impressive 85% to 95% when this fluid was used, with the highest recovery percentage recorded with NANOSEAL KP drilling fluid. This suggests that NanoSeal-KP is an effective option for maintaining shale stability during drilling operations in the area of study (Figure 11).

Table 1: Drilling fluids formulation

	Drilling Fluids Formulations															
Product	KCl-Polymer Mud				High-Performance WBM				NanoSeal – KP				LTOBM			
Sample Composition	Field (ppb)	Lab gram	Mix Order	Time (min)	Field PPb	Lab gram	Mix Order	Time (min)	Field PPb	Lab gram	Mix Order	Time (min)	Field PPb	Lab gram	Mix Order	Time (min)
Water	301.146	301.146	1	-	276.34	276.34	1	-	270.26	270.26	1	-	68.75	68.75	4	-
Caustic Soda	1	1	2	1	-	-	-	-	-	-	-	-	-	-	-	-
Soda Ash	1	1	3	1	1	1	2	1	1	1	2	1	-	-	-	-
Sodium Chloride (Salt)	40.4	40.4	4	3	40	40	3	3	40	40	3	3	-	-	-	-
Potassium Chloride (KCl)	25.71	25.71	5	3	25	25	4	3	25	25	4	3	-	-	-	-
Modified HT Starch	4	4	6	5	5	5	5	5	4	4	5	5	-	-	-	-
Polly Anionic Cellulose (PAC)	6	6	7	5	6	6	6	5	6	6	6	5	-	-	-	-
Xanthan Gum (Viscosifier)	1	1	8	5	1	1	7	5	1	1	7	5	-	-	-	-
Dry Acrylic Acid	-	-	-	-	4	4	8	5	4	4	8	5	-	-	-	-
Liquid Polyamine	-	-	-	-	14.28	14.28	9	3	14.28	14.28	9	3	-	-	-	-
Liquid Lubricant	-	-	-	-	6.44	6.44	10	1	6.44	6.44	10	1	-	-	-	-
NanoSeal (Latex)	-	-	-	-	-	-	-	-	7	7	11	3	-	-	-	-
Solid lubricant agent	-	-	-	-	-	-	-	-	5	5	12	5	-	-	-	-
Calcium Carbonate (F/M)	40	40	9	3	40	40	11	3	40	40	13	3	40	40	7	5
Base Oil	-	-	-	-	-	-	-		-	-	-	-	166.53	166.53	1	-
Lime	-	-	-	-	-	-	-	-	-	-	-	-	10	10	2	2
Emulsifier Package	-	-	-	-	-	-	-	-	-	-	-	-	9	9	3	3
Calcium Chloride (CaCl2)	-	-	-	-	-	-	-	-	-	-	-	-	40.1	40.1	4	15
Organophilic Clay	-	-	-	-	-	-	-	-	-	-	-	-	5	5	5	5
Polymeric HTHP Control	-	-	-	-	-	-	-	-	-	-	-	-	2	2	6	5
Barite (API)	-	-	-	-	-	-	-	-	-	-	-	-	76.59	76.59	8	5

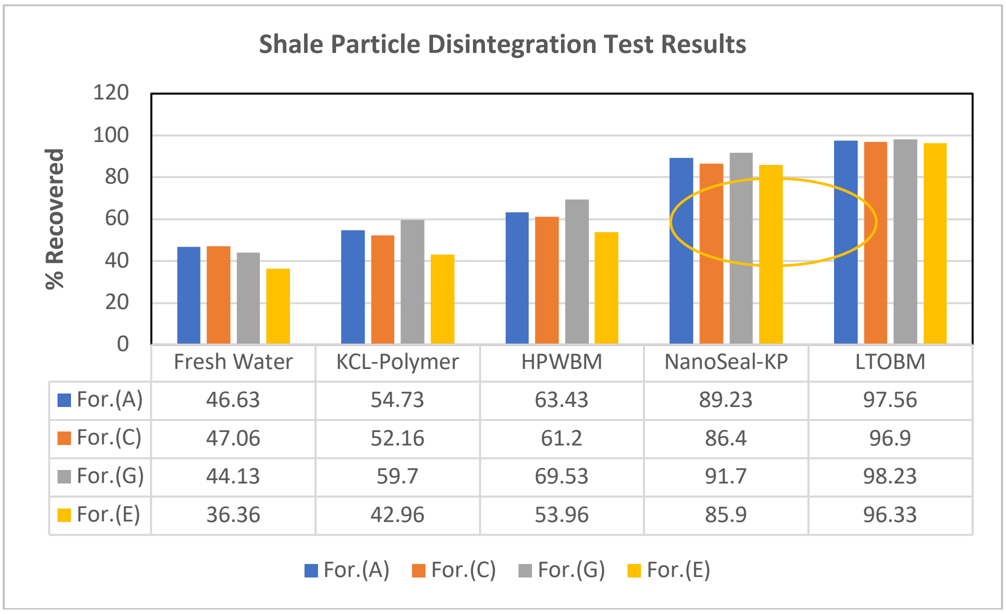

Figure 11: The SPDT on formation A, C, G, and E.

3.5. Accretion Test

Based on the results of the accretion test, it can be observed that the four shale samples studied (formations A, C, G, and E) consistently performed similarly to previous tests. These tests showed that these shale samples had the highest accretion percentage when tested with fresh water and the lowest when tested with LTOBM. Additionally, it was found that the E shale sample displayed higher reactivity compared to the other samples (Figure 12). When comparing the different mud systems used, the High-Performance WBM performed better than fresh water and KCl-polymer mud in inhibiting shale cuttings. However, the innovative fluid (NanoSeal-KP) demonstrated superior performance and premium inhibition of shale cuttings, with acceptable results comparable to LTOBM.

Table 2: Drilling fluids parameters

Experiment		**KCl-Polymer Mud**		**High-Performance WBM**		**NanoSeal – KP**		**LTOBM**	
Period Aged	Hours	-	16	-	16	-	16	-	16
Temperature	°F	-	160	-	160	-	160	-	160
Dynamic/Static	D/S	Initial	D	Initial	D	Initial	D	Initial	D
Mud Density	ppg	10.0	10.0	10.0	10.0	10.0	10.0	10.0	10.0
RHEOLOGY:	Temp. °F	120	120	120	120	120	120	150	150
600	RPM	110	81	130	90	150	120	100	80
300	RPM	74	51	86	60	100	80	75	60
200	RPM	64	41	76	50	90	70	65	50
100	RPM	54	31	66	41	80	60	45	40
6	RPM	12	8	15	10	16	12	15	12
3	RPM	11	7	13	9	15	11	13	11
Gel 10 Sec	lbs/100ft^2	11	7	13	9	15	11	20	15
Gel 10 Min	lbs/100ft^2	14	10	18	14	20	15	27	21
Plastic Viscosity	Cp	36	30	44	30	50	40	25	20
Yield Point	lbs/100ft^2	38	21	42	30	50	40	50	40
LSYP	lbs/100ft^2	10	6	11	8	14	10	11	10
HTHP	Cc/30min	10	25	8	16	5	10	2	5
API Filter Press	Cc/30min	8	18	5	8	4	7	-	-
Salinity	Mg/l	137200	137200	137200	137200	137200	137200	-	-
PH		10	9	10	10	10	10	-	-
Coefficient of Friction		0.12854	0.12854	0.09594	0.09594	0.03211	0.03211	0.06285	0.06285
Electrical Stability	Volt	NA	-	-	-	-	-	550	440
POM	Ml	NA	-	-	-	-	-	4.2	3.9
Excess Lime	ppb	NA	-	-	-	-	-	5.46	5.07
CaCl2	%	NA	-	-	-	-	-	35	35
Water Phase Salinity		NA	-	-	-	-	-	288k	288k
Retort (Water/Oil/Solid)	%	NA	-	-	-	-	-	22/67/11	22/67/11
Oil: Water Ratio		NA	-	-	-	-	-	75/25	75/25

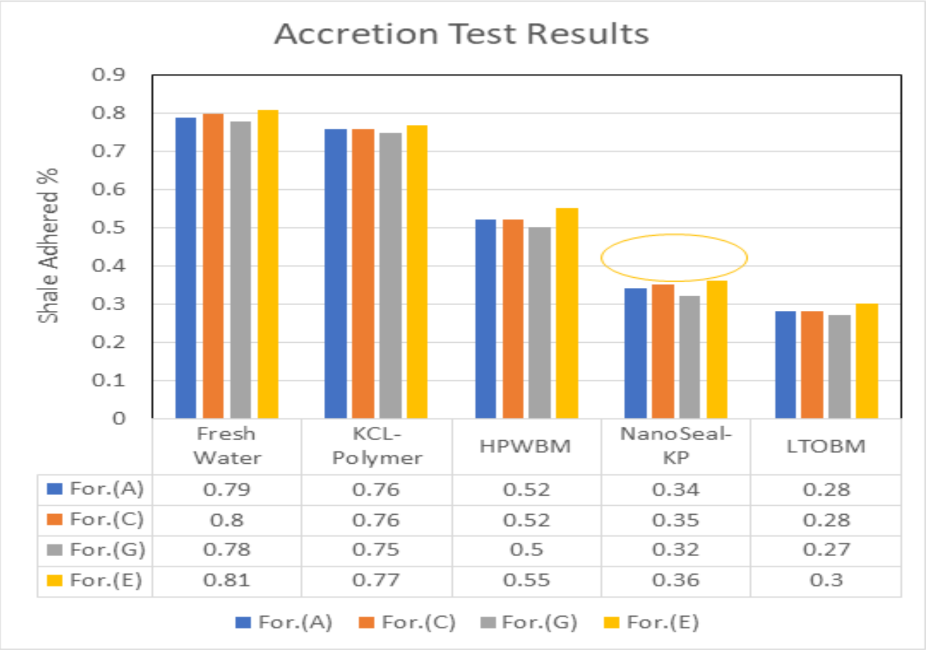

	Fresh Water	KCL-Polymer	HPWBM	NanoSeal-KP	LTOBM
For.(A)	0.79	0.76	0.52	0.34	0.28
For.(C)	0.8	0.76	0.52	0.35	0.28
For.(G)	0.78	0.75	0.5	0.32	0.27
For.(E)	0.81	0.77	0.55	0.36	0.3

Figure 12: Results of the Accretion test on formations A, C, G, and E.

Table 3 – results of shale disintegration test (SPDT) test on (A) shale formation.

Shale Recovery	Units	Water	KCL-Polymer	HPWBM	NanoSeal - KP	LTOBM
Initial Weight (2-4 mm)	gm	30	30	30	30	30
Weight of the Wet Chippings (2-4 mm)	gm	24.8	24.1	27.1	28	28.56
Weight of the Wet Chippings (1-2 mm)	gm	2.8	2.45	2.95	2.99	2.68
Total Weight of the Wet Chippings	gm	27.6	26.55	30.05	30.99	31.24
Final Weight (dry chippings)	gm	13.99	16.42	19.03	26.84	29.27
Cuttings Recovery	**%**	46.63	54.73	63.43	89.46	97.56
Moisture of Recovered Sample	%	49.31	38.15	36.67	13.39	6.30

Table 4 – results of shale disintegration test (SPDT) test on (C) shale formation.

Shale Recovery	Unit	Water	KCL-Polymer	HPWBM	NanoSeal - KP	LTOBM
Initial Weight (2-4 mm)	gm	30	30	30	30	30
Weight of the Wet Chippings (2-4 mm)	gm	26.52	27.21	27.8	28.41	28.4
Weight of the Wet Chippings (1-2 mm)	gm	2.71	3	2.72	2.65	2.69
Total Weight of the Wet Chippings	gm	29.23	30.21	30.52	31.06	31.09
Fina Weight (dry chippings)	gm	14.12	15.65	18.36	25.92	29.07
Cuttings Recovery	**%**	47.06	52.16	61.2	86.4	96.9
Moisture of Recovered Sample	%	51.69	48.195961	39.84	16.54	6.49

Table 5 – results of shale disintegration test (SPDT) test on (G) shale formation.

Shale Recovery	Unit	Water	KCL-Polymer	HPWBM	NanoSeal - KP	LTOBM
Initial Weight (2-4 mm)	gm	30	30	30	30	30
Weight of the Wet Chippings (2-4 mm)	gm	28.91	28.81	28.23	28.41	28.7
Weight of the Wet Chippings (1-2 mm)	gm	2.63	2.75	3	2.85	2.8
Total Weight of the Wet Chippings	gm	31.54	31.56	31.23	31.26	31.5
Fina Weight (dry chippings)	gm	13.24	17.91	20.86	27.51	29.47
Cuttings Recovery	%	44.13	59.7	69.53	91.7	98.23
Moisture of Recovered Sample	%	58.02	43.25	33.20	11.99	6.44

Table 6 – results of shale disintegration test (SPDT) test on (E) shale formation.

Shale Recovery	Unit	Water	KCL-Polymer	HPWBM	NanoSeal - KP	LTOBM
Initial Weight (2-4 mm)	gm	30	30	30	30	30
Weight of the Wet Chippings (2-4 mm)	gm	23.24	22.7	23.89	28.49	28.66
Weight of the Wet Chippings (1-2 mm)	gm	2.36	2.45	2.99	2.68	2.34
Total Weight of the Wet Chippings	gm	25.6	25.15	26.88	31.17	31
Fina Weight (dry chippings)	gm	10.91	12.89	16.19	25.77	28.9
Cuttings Recovery	%	36.36	42.96	53.96	85.9	96.33
Moisture of Recovered Sample	%	57.38	48.74	39.76	17.32	6.77

3.6. Bulk Hardness Test

Bulk hardness testing is considered an extension of the Shale Particle Disintegration Test (SPDT). Highly efficient shale inhibitors provide harder shale cuttings and higher torque readings. The bulk hardness curves generated from this testing reveal a marginal difference in profile for inhibited WBM drilling fluids. Compared to these inhibited fluids, LTOBM and Freshwater appear markedly different.

Figures 13-16 illustrate the test results and comparison of Freshwater, KCL-polymer, HPWBM, NanoSeal-KP, and LTOBM for A, C, G, and E formations, respectively. The NanoSeal-KP uses an innovative nano-sized particle sealing agent. Overall, bulk hardness testing provides valuable insights for assessing cuttings' stability, and its application as an extension to cuttings disintegration testing is worth considering.

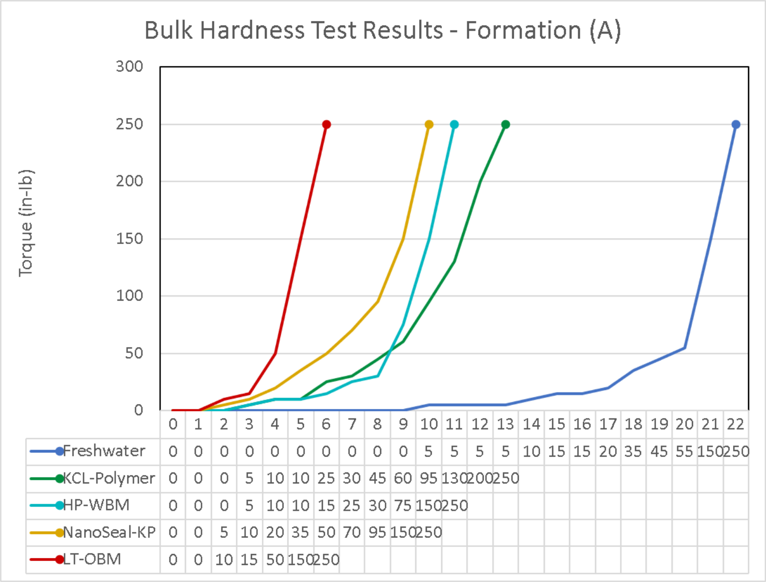

	0	1	2	3	4	5	6	7	8	9	10	11	12	13	14	15	16	17	18	19	20	21	22
Freshwater	0	0	0	0	0	0	0	0	0	0	5	5	5	5	10	15	15	20	35	45	55	150	250
KCL-Polymer	0	0	0	5	10	10	25	30	45	60	95	130	200	250									
HP-WBM	0	0	0	5	10	10	15	25	30	75	150	250											
NanoSeal-KP	0	0	5	10	20	35	50	70	95	150	250												
LT-OBM	0	0	10	15	50	150	250																

Figure 13: Bulk hardness output curves for (A) shale samples tested with five different fluids

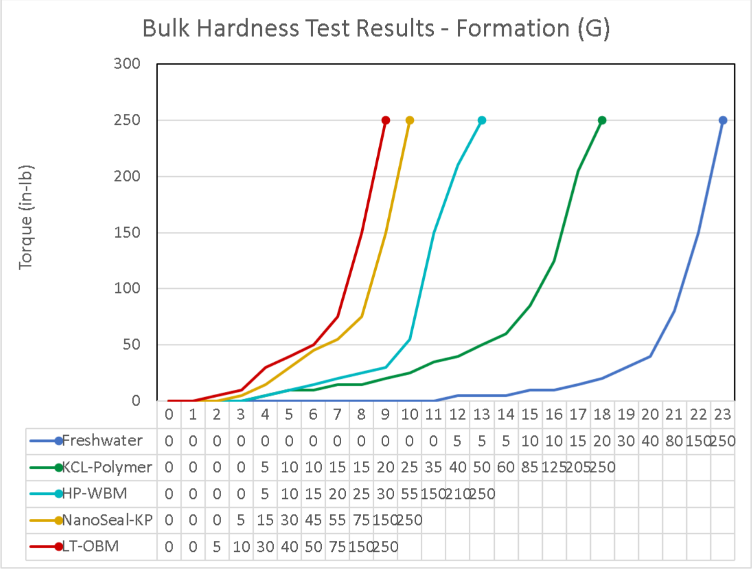

	0	1	2	3	4	5	6	7	8	9	10	11	12	13	14	15	16	17	18	19	20	21	22	23
Freshwater	0	0	0	0	0	0	0	0	0	0	0	0	5	5	5	10	10	15	20	30	40	80	150	250
KCL-Polymer	0	0	0	0	5	10	10	15	15	20	25	35	40	50	60	85	125	205	250					
HP-WBM	0	0	0	0	5	10	15	20	25	30	55	150	210	250										
NanoSeal-KP	0	0	0	5	15	30	45	55	75	150	250													
LT-OBM	0	0	5	10	30	40	50	75	150	250														

Figure 14: Bulk hardness output curves for (C) shale samples tested with five different fluids

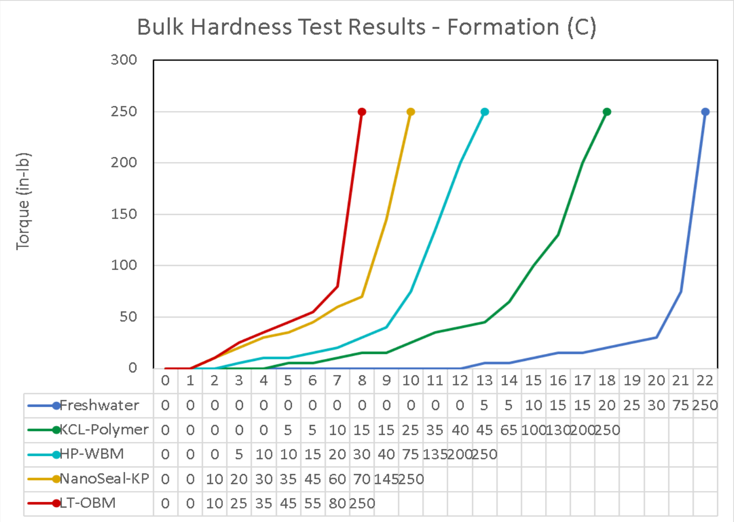

	0	1	2	3	4	5	6	7	8	9	10	11	12	13	14	15	16	17	18	19	20	21	22
Freshwater	0	0	0	0	0	0	0	0	0	0	0	0	0	5	5	10	15	15	20	25	30	75	250
KCL-Polymer	0	0	0	0	0	5	5	10	15	15	25	35	40	45	65	100	130	200	250				
HP-WBM	0	0	0	5	10	10	15	20	30	40	75	135	200	250									
NanoSeal-KP	0	0	10	20	30	35	45	60	70	145	250												
LT-OBM	0	0	10	25	35	45	55	80	250														

Figure 15: Bulk hardness output curves for (G) shale samples tested with five different fluids.

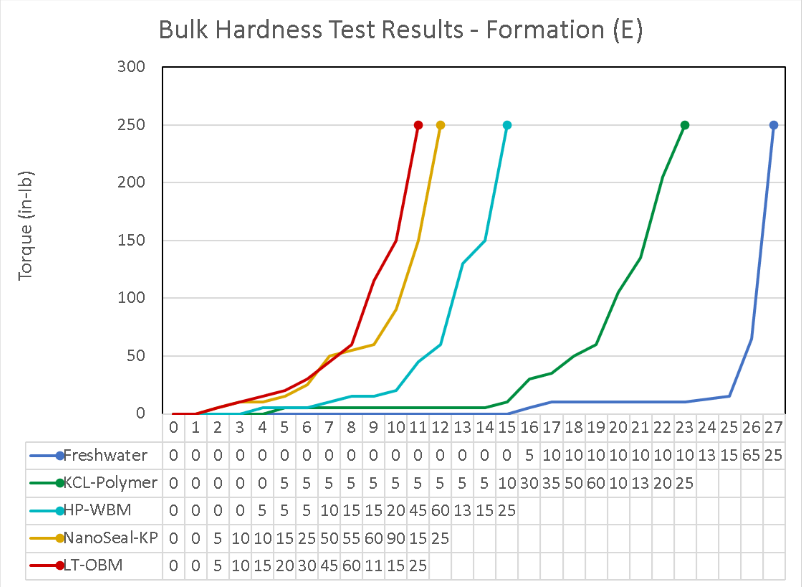

	0	1	2	3	4	5	6	7	8	9	10	11	12	13	14	15	16	17	18	19	20	21	22	23	24	25	26	27
Freshwater	0	0	0	0	0	0	0	0	0	0	0	0	0	0	0	0	5	10	10	10	10	10	10	10	13	15	65	25
KCL-Polymer	0	0	0	0	0	5	5	5	5	5	5	5	5	5	5	10	30	35	50	60	10	13	20	25				
HP-WBM	0	0	0	0	5	5	5	10	15	15	20	45	60	13	15	25												
NanoSeal-KP	0	0	5	10	10	15	25	50	55	60	90	15	25															
LT-OBM	0	0	5	10	15	20	30	45	60	11	15	25																

Figure 16: Bulk hardness output curves for (E) shale samples tested with five different fluids.

3.7. Linear Swelling Meter Test (LSM)

A Linear Swell Meter test, also known as LSM, was carried out on four rock samples known as 'A', 'C', 'G', and 'E' formations. These rock samples were specifically chosen from their respective formations as they were deemed to be the most challenging ones based on CEC and SEM analysis. The test used all possible drilling fluids to ensure the most accurate results.

Formation-A LSM

During the LSM test, various types of drilling fluids were used to expose shale samples for a period of 36 hours. The linear swelling of the shale was measured using the OFITE dynamic linear swell meter tester. Figure 17 provides the results of the formation (A) shale swelling using different drilling fluids, including water, KCL/Polymer mud, High-Performance Water-Based Mud, NanoSeal – KP (an innovative fluid), and Low-Toxic Oil-Based Mud (LTOBM).

Upon interaction with different fluids, shale wafers exhibited immediate swelling for all utilized fluids. Fresh water and KCL/Polymer had the maximum swelling rate in the first 6 hours, followed by a moderate rate for 12 more hours. Conversely, the HPWBM and NanoSeal – KP showed a moderate trend from the beginning of the experiment, and all water-based fluids stabilized approximately after 24 hours of exposure, except the HPOWBM, which showed a swelling behavior for a complete 33 hours. The LTOBM, however, showed a low swelling behavior for only the first 0.3 hours, after which the curve stabilized until the end of the experiment, after 36 hours.

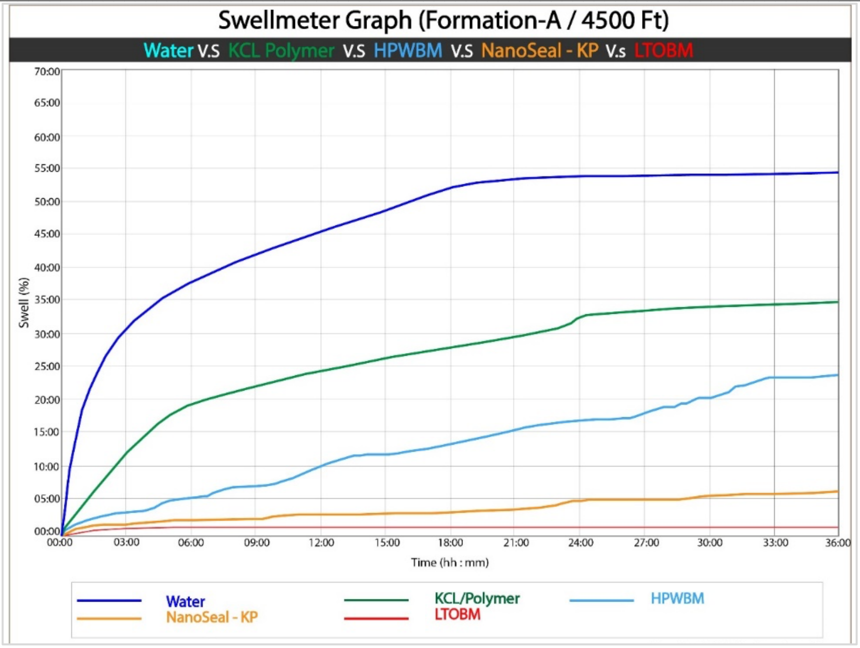

Figure 17: Results of linear swell meter experiments for formation (A) shale sample using different drilling fluids.

Formation-C LSM

During the LSM test Formation (C), the formation of shale was examined using various types of drilling fluids for 36 hours. The linear swelling of the shale was identified through the OFITE dynamic linear swell meter tester. Figure 18 displays the outcome of the LSM examination conducted with various drilling fluids, including water, KCL/polymer mud, High-Performance Water-Based Mud, NanoSeal – KP, and Low Toxic Oil-Based Mud (LTOBM).

An immediate swelling of the shale wafers was caused by all fluids. The highest swelling rate for the first 24 hours was observed in fresh water and KCL/polymer, followed by a stability for the next twelve hours. On the other hand, HPWBM and NanoSeal – KP showed a moderate trend for the first 24 hours and then stabilized until the end of the experiment. LTOBM, however, exhibited a low swelling behavior for the first 3 hours, after which it remained stable until the end of the 36-hour experiment.

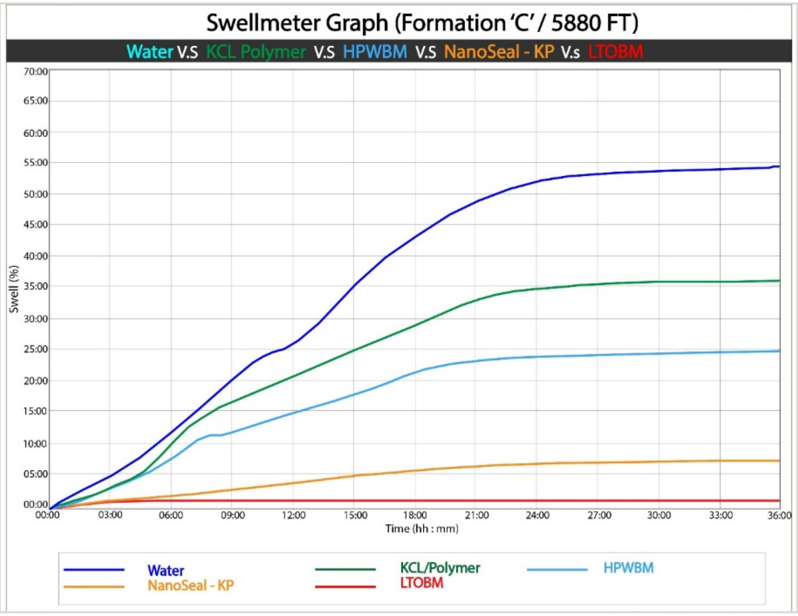

Figure 18: Results of linear swell meter experiments for (C) formation shale sample using different drilling fluids.

Formation-G LSM

The (G) formation was tested with various drilling fluids for 36 hours to analyze its linear swelling using the OFITE dynamic linear swell meter tester. Figure 19 displays the results of the test for different fluids such as Fresh Water, KCL/Polymer mud, High-Performance Water-Based Mud, NanoSeal – KP, and Low Toxic Oil-Based Mud (LTOBM).

During the experiment, the shale wafers showed immediate swelling with all fluids. Freshwater had the highest swelling rate for the first 21 hours, followed by a moderate rate for the next 9 hours, where the curve stabilized till the end of the experiment after 36 hours. The KCL-POLYMER and HPWBM showed a moderate trend at the first 27 hours, then the curve stabilized till the end of the experiment. On the other hand, the NanoSeal – KP showed a low trend from the beginning and stabilized after 24 hours. LTOBM exhibited very low swelling behavior for the first 1.5 hours, after which the curve stabilized until the end of the experiment, after 36 hours.

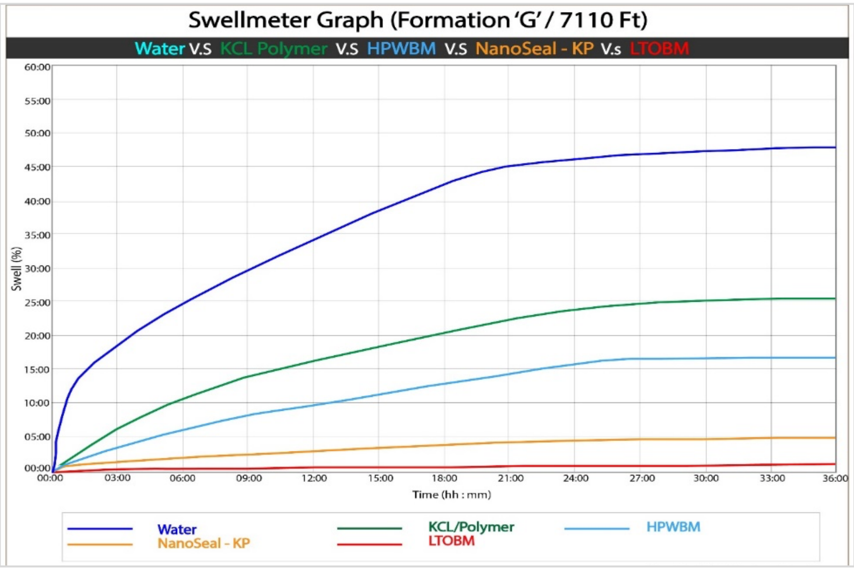

Figure 19: results of linear swell meter experiments for 'G' formation shale sample using different drilling fluids.

Formation-E LSM

During the LSM test, (E) formation was examined using various types of drilling fluids for 36 hours. The linear swelling of the shale was identified through the OFITE linear swell meter tester. Results of the LSM using different drilling fluids, such as water, KCL/polymer mud, High-Performance Water-Based Mud, NanoSeal – KP, and Low Toxic Oil-Based Mud (LTOBM), were showcased in Figure 20.

Immediate swelling was observed in the shale wafers upon interaction with different fluids. The highest swelling rate in the first 26 hours was observed for fresh water and KCL/Polymer, which was followed by a slow swelling rate until the end of the experiment. HPWBM showed a moderate trend from the beginning until the end of the experiment, after 36 hours. NanoSeal – KP showed a low swelling trend from the start of the experiment and stabilized after 21 hours of exposure. The LTOBM, however, showed a very low swelling behavior for only the first 2 hours, after which the curve stabilized until the end of the experiment, after 36 hours.

Overall, these results provide valuable insights into the behavior of different drilling fluids when interacting with shale samples, which is essential for optimizing drilling operations and ensuring their effectiveness and safety. Figure 21 provides the experimental results for all utilized shale samples.

Superior inhibition properties for all tested samples were demonstrated by NanoSeal-KP, as depicted in Figure 21. It was found to exhibit significantly remarkable results compared to high-performance water-based mud and comparable results to low-toxicity oil-based mud.

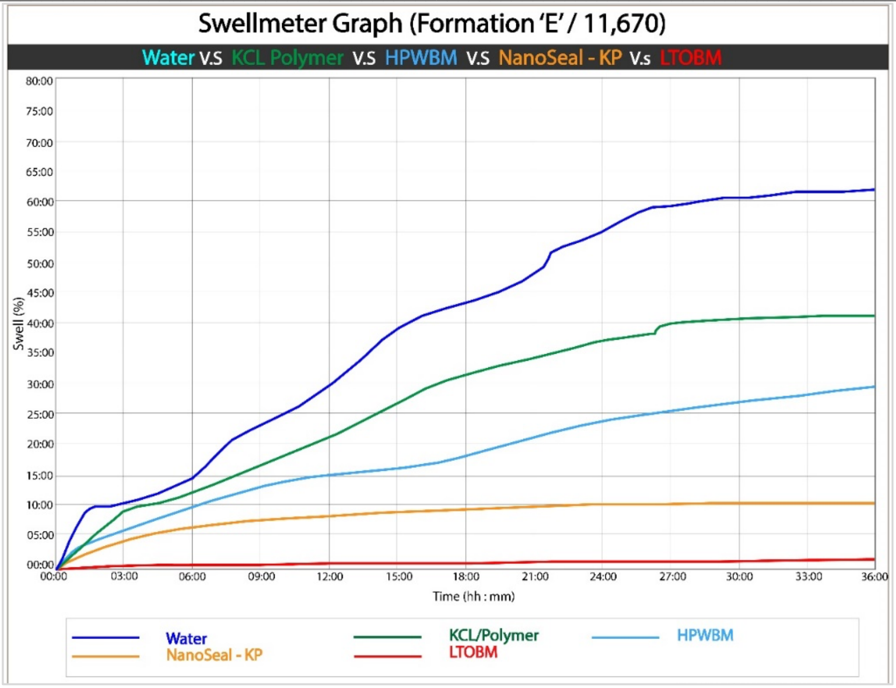

Figure 20: Results of linear swell meter experiments for (E) formation shale sample using different drilling fluids.

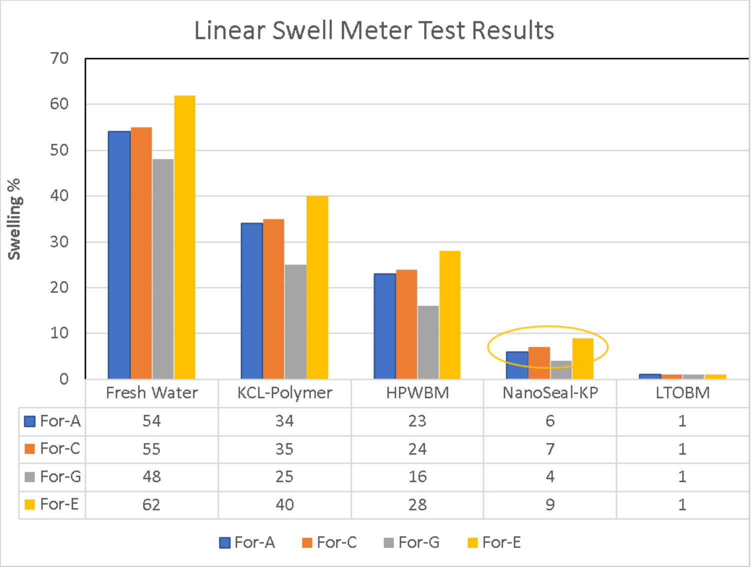

	Fresh Water	KCL-Polymer	HPWBM	NanoSeal-KP	LTOBM
For-A	54	34	23	6	1
For-C	55	35	24	7	1
For-G	48	25	16	4	1
For-E	62	40	28	9	1

Figure 21: The LSM results for a comprehensive set of shale samples, including formation A, C, G, and E.

4. Conclusion:

The findings suggest that most instability encountered during drilling operations in the Western Desert, specifically in field X, resulted from inadequate rock-fluid interaction and pore pressure transmission rather than mechanical factors. In the context of this study, field-X refers to a specific oil field located in the Western Desert region. Therefore, the chemical analysis of drilling fluids and their compatibility with shale formations was considered a key factor in preventing drilling problems and eliminating non-productive time (NPT) during drilling operations.

These recommendations include using various types and combinations of shale inhibitors and solid lubricant materials to optimize drilling fluid compositions and properties, achieving both wellbore stability and operational efficiency. The results also highlight the importance of accurate and reliable models for predicting chemical instability in the wellbore, aiding in developing effective wellbore stability management strategies.

The experimental findings reveal that chemical instability in drilled formations significantly contributes to wellbore instability in the study area. The interaction between fluids and shale formations causes swelling, disintegration, and alteration of rock properties, leading to wellbore instability. The degree of instability may differ depending on the specific composition and characteristics of both the drilling fluids and the shale formations.

This research provides valuable insights into the interaction between drilled rock and drilling fluid in oil and gas wells in the Western Desert of Egypt and its effects on wellbore stability and the drilling process. By enhancing our understanding and developing effective strategies for managing wellbore stability and optimizing drilling processes in the Western Desert, this work aims to improve oil and gas operations' safety, efficiency, and success.

The phenomenon of mud pressure diffusion into the near-wellbore zone, followed by an increase in near-wellbore pore pressure, can result in instability over an extended period. To effectively prevent this, OBM/SBM leverages capillary forces. However, WBM is susceptible to this issue when it encounters low-permeability shales while operating at overbalance conditions.

To improve the efficacy of WBM in environmentally sensitive regions, a micro-fracture sealant of nano size can be employed. This sealant reduces pore pressure transmission, leading to a significant enhancement in WBM performance. Consequently, WBM becomes a sustainable alternative that can rival OBM/SBM in both efficiency and environmental impact.

5. Conflicts of interest

There are no conflicts to declare.

6. Acknowledgment

We would like to express our sincere gratitude to the editorial team of the Egyptian Journal of Chemistry for their valuable efforts throughout the publication process. We are also grateful to Hani Khalil for his unwavering support and assistance. Furthermore, we extend our appreciation to Mohamed Tariq and Magdy Abdelazim Youssef for their invaluable support during the lab testing process. Their expertise and assistance were instrumental in the successful completion of this study

7. References

1. van Oort, E., et al., *Transport in shales and the design of improved water-based shale drilling fluids.* SPE drilling & completion, 1996. **11**(03): p. 137-146.
2. Chenevert, M.E., *Shale control with balanced-activity oil-continuous muds.* Journal of Petroleum technology, 1970. **22**(10): p. 1309-1316.
3. Gholami, R., et al., *A review on borehole instability in active shale formations: Interactions, mechanisms and inhibitors.* Earth-Science Reviews, 2018. **177**: p. 2-13.
4. Steiger, R.P. and P.K. Leung, *Quantitative determination of the mechanical properties of shales.* SPE drilling engineering, 1992. **7**(03): p. 181-185.
5. Chuprin, M., et al. *Evaluation of tuscaloosa marine shale stability using capillary suction time and roller oven tests*. in *SPE/AAPG/SEG Unconventional Resources Technology Conference*. 2020. URTEC.
6. Mody, F.K. and A.H. Hale, *Borehole-stability model to couple the mechanics and chemistry of drilling-fluid/shale interactions.* Journal of petroleum technology, 1993. **45**(11): p. 1093-1101.
7. Sone, H. and M.D. Zoback, *Mechanical properties of shale-gas reservoir rocks—Part 1: Static and dynamic elastic properties and anisotropy.* Geophysics, 2013. **78**(5): p. D381-D392.
8. van Oort, E., et al. *Critical parameters in modelling the chemical aspects of borehole stability in shales and in designing improved water-based shale drilling fluids*. in *Drilling and general petroleum engineering*. 1994.
9. Mohiuddin, M., et al., *Analysis of wellbore instability in vertical, directional, and horizontal wells using field data.* Journal of petroleum Science and Engineering, 2007. **55**(1-2): p. 83-92.
10. Ferreira, C.C., et al., *Partially hydrophobized hyperbranched polyglycerols as non-ionic reactive shale inhibitors for water-based drilling fluids.* Applied Clay Science, 2016. **132**: p. 122-132.
11. Al-Arfaj, M.K. *An Experimental Study on Shale-Fluid Interactions to Help Drill Stable Shale Formations*. in *International Petroleum Technology Conference*. 2022. IPTC.
12. Ahmad, H.M., et al. *Improving the drilling fluid properties using nanoparticles and water-soluble polymers*. in *SPE Kingdom of Saudi Arabia annual technical symposium and exhibition*. 2017. OnePetro.
13. Chenevert, M. and M. Amanullah, *Shale preservation and testing techniques for borehole-stability studies.* SPE Drilling & Completion, 2001. **16**(03): p. 146-149.
14. Chenevert, M. and M. Amanullah. *Assessment of the degree of water saturation in shales*. in *Rock mechanics tools and techniques*. 1996.
15. Amanullah, M., *Shale-drilling mud interactions*. 1993, Department of Mineral Resources Engineering, Imperial College.
16. Forsans, T.M. and L. Schmitt. *Capillary forces: The neglected factor in shale instability studies?* in *SPE/ISRM Rock Mechanics in Petroleum Engineering*. 1994. SPE.
17. Seed, H.B. and C. Chan, *Undrained strength of compacted clays after soaking.* Journal of the Soil Mechanics and Foundations Division, 1959. **85**(6): p. 31-47.
18. Amanullah, M., J. Marsden, and H. Shaw. *Effects of rock-fluid interactions on the petrofabric and stress-strain behaviour of mudrocks*. in *SPE/ISRM Rock Mechanics in Petroleum Engineering*. 1994. SPE.
19. Fredlund, D. and H. Rahardjo, *Soil mechanics for unsaturated soils John Wiley & Sons Inc.* New York (USA), 1993.
20. Chittoori, B. and A.J. Puppala, *Quantitative estimation of clay mineralogy in fine-grained soils.* Journal of Geotechnical and Geoenvironmental engineering, 2011. **137**(11): p. 997-1008.
21. *API RP 13I, Recommended Practice for Laboratory Testing of Drilling Fluids, Ninth Edition. 2020. Washington DC. API.*
22. Mukhopadhyay, S.M., *Sample preparation for microscopic and spectroscopic characterization of solid surfaces and films.* Sample preparation techniques in analytical chemistry, 2003. **162**: p. 377-411.
23. van Oort, E., et al. *How to test fluids for shale compatibility*. in *The AADE Fluids Technical Conference and Exhibition. American Association of Drilling Engineers, Houston, USA*. 2016.
24. Patel, A., et al. *Advances in inhibitive water-based drilling fluids–can they replace oil-based muds?* in *International Symposium on Oilfield Chemistry*. 2007. OnePetro.
25. Patel, A.D. *Design and development of quaternary amine compounds: shale inhibition with improved environmental profile*. in *SPE international symposium on oilfield chemistry*. 2009. OnePetro.

26. Stephens, M., et al. *AADE 2009-NTCE-11-04: Laboratory Methods to Assess Shale Reactivity with Drilling Fluids*. 2009. National technical conference & exhibition New Orleans, Lousiana, USA.
27. OFITE, *OFITE. 2018. Dynamic Linear Swell Meter 150-80-1 - Instruction Manual. Revision 6. Houston, Texas, USA.*
28. *API RP 13B-1, Recommended Practice for Field Testing Water-Based Drilling Fluids, Fifth Edition. 2019. Washington DC. API.*
29. *API RP 13B-2, Recommended Practice for Field Testing Oil-based Drilling Fluids, Fifth Edition. 2014. Addendum. 2019. Washington DC. API.*